JOINT EUROPEAN TORUS JET

JET–P(86)42

H.P. Summers, K.H. Behringer, A. Boileau, M.J. Forrest, L. Horton,
N.J. Peacock, M.F. Stamp and M. von Hellerman

Interpretation of Emission from Ions Out of Ionisation Balance

Interpretation of Emission from Ions Out of Ionisation Balance

H.P. Summers, K.H. Behringer, A. Boileau, M.J. Forrest, L. Horton, N.J. Peacock, M.F. Stamp and M. von Hellerman

JET-Joint Undertaking, Culham Science Centre, OX14 3DB, Abingdon, UK

ABSTRACT.

Ion population which appear out of ionisation balance are often observed in laboratory plasmas. Spatially or temporally, they mark the disequilibrium between atomic processes in the presence of strong certain spectrum line combinations can serve as diagnostic indicators which characterise the dynamic state from an atomic point of view.

This paper establishes indicators for two cases, namely

(a) transiently ionising ions in low stages of ionisation. This is applied to the impurity influx from the walls and limiters of the JET tokamak

(b) transiently recombining highly ionised or stripped ions. This is applied to impurity recombination in the JET plasma in the presence of neutral hydrogen beams.

1. INTRODUCTION

JET tokamak discharges, because of recycling at material boundaries and supplementary heating produce plasma environments in which impurity ions radiate unusually. This is in comparison with typical astrophysical plasmas where ions are mostly observed radiating in a near ionisation equilibrium environment. Two cases in JET which have prompted new theoretical atomic physics investigation are observations of near neutral impurity ions in the vicinity of limiting surfaces, and observations of 'charge exchange recombination lines' from nearly stripped impurity ions in neutral hydrogen heating beam irradiated volumes. The electron temperature in the immediate vicinity of the limiting surfaces of the plasma (carbon limiters, inner wall carbon protection tiles and ICRH antenna screens) is typically ~ 50-100 eV. This is a strongly ionising environment for a neutral impurity atom entering the plasma from the limiting surface. It ionises through several ionisation stages while still near the surface. Observations of spectrum line radiation from such ions along a line of sight directed at the surface can be interpreted as impurity fluxes from the surface (Behringer, 1986). Relevant impurities in JET are carbon, oxygen, chromium and nickel and for these elements observations can conveniently be made in visible or quartz UV wavelengths.

By contrast, in the centre of JET at typical temperatures Te ~ 4 KeV, the light impurities carbon and oxygen are stripped to the bare nucleus stage. When neutral hydrogen heating beams are switched on however, a strongly recombining environment is established in which a direct charge exchange reaction

$$A^{+z}o + H(1s) \rightarrow A^{+z}o^{-1} \ (nl) + p$$

populates high n levels. The subsequent cascade radiation called 'charge exchange recombination radiation' is characteristic (see Peacock - this conference). It can

generally be observed at visible wavelengths and may be interpreted in terms of central impurity ion temperatures, plasma rotation and abundances (Von Hellerman et al., 1986). In this paper we describe in turn some features of the atomic analysis of these two cases.

2. INFLUX ANALYSIS

A significant proportion of inflowing ions are in metastable states. For example, O^{+1} with ground term $2s^2 2p^3\ ^4S$ has metastable states $2s^2 2p^3\ ^2D$ and $2s^2 2p^3\ ^2P$, and typically one half of the O^{+1} population is in the metastable states. Substantial metastable ion populations are usual in low density astrophysical plasmas. However in the tokamak case, there is not a local statistical equilibrium balance of ground and metastable populations of each ionisation stage at the electron temperature and density. Ionisation rates are sufficiently large relative to excitation and radiative rates that metastable populations are dependent on their direct birth through ionisation (possibly inner shell or excitation/autoionisation) from the stage below. This metastable population 'freezing' is illustrated in figure 1. Consequently influx in each populated metastable state must be determined separately. Net influx of an element may be derived from spectral intensity measurements on lines from any ionisation stage of the element which ionises locally near the surface. For an ionisation stage with metastables σ: $\sigma=1, \ldots, m$, m linearly independent lines must be measured. The flux of element A, Γ_A then may be written as

$$\Gamma_A = \sum_{\sigma,\rho=1}^{m} \{Ne\ S_\sigma\ W^{-1}_{\sigma\rho}\} I\rho$$

where $S\sigma$ is the ionisation rate coefficient for metastable σ and the matrix elements $W^{-1}_{\sigma\rho}$ depend on the collisional - radiative processes involved in exciting the spectrum lines (Behringer et al. (1987) - to be published). The expression in { } brackets is a number of ionisations/photon and is

calculated from theoretical atomic physics. For a single ground state and single line in the zero density limit $W_{\sigma\rho}^{-1}$ simplifies to the reciprocal of the electron density times an excitation rate coefficient times a radiative branching ratio. $I\rho$ is the column emissivity of spectrum line ρ, that is, integrated along a line of sight directed at the surface. The calculation procedures for the theoretical quantities are rather different for light ions and transition metals. For C^{+1}, C^{+2}, O^{+1} and O^{+2}, the ground and metastable states have n=2 valence shells. Visible spectrum lines however occur only in n=3-3 or higher transitions. Also the visible lines are observable only if there is no strong competing radiative branch to the n=2 levels. For example, the levels which must be included in the excited population calculation (to determine $W_{\sigma\rho}^{-1}$) for O^{+1} is shown in figure 2, with the lines used for JET analysis highlighted. Three points are of note, namely, (a) the primary electron collisional excitation to the radiating level is non-dipole, (b) there is significant cascade correction from 4d, 5d, ... levels to the 3p populations since the excitation rates to these higher levels are allowed and large, (c) two electron jump radiative transitions compete with the observed 3p-3s radiative transitions. Rates for many of these processes are not confidently known. We have used a variety of sources together with some at initio calculations of our own, but uncertainties are large. Figure 3 shows the behaviour of some of the excited level populations of O^{+1} with density. Tokamaks such as JET are in the low density regime. Figure 4 shows some theoretical ionisation/photon results for the low density limit.

Neutral and singly ionised metals have a complex set of ground and metastable levels classified by parentage and grand parentage. Dipole allowed line emissions are of the form $3d^q$-$3d^{q-1}$ 4p, $3d^{q-1}$ 4s-$3d^{q-1}$ 4p and $3d^{q-2}$ $4s^2$-$3d^{q-2}$ 4s4p, and are generally at visible or quartz UV wavelengths. Figure 5 illustrates the configuration and relevant term structure for Cr^{+1}. Table 1 shows the metastable states of interest. The metastable state populations shown may be

investigated via the indicated lines. Upper states tend to have impure parentage and so there is some branching from the upper levels, also in some cases an upper level may be strongly excited from more than one metastable. There is a serious deficiency of necessary atomic rate data for the ionisation/photon deduction. Assessed f-value data is incomplete and no refined collisional data is available. We have made extensive use of semi-empirical f-values and simple approximations for allowed collisional excitations. Figure 6 shows preliminary ionisation/photon results for Cr^{+1}.

Table 2 presents some derived impurity fluxes for JET limiters based on the above theoretical data. Broad continuity of flux in different stages is achieved. With refinement of theoretical data, a more ambitious resolution of state selective ionisation (metastable to metastable) and deduction of 'at wall' neutral impurity state will be possible.

3. CHARGE EXCHANGE LINE ANALYSIS

Suitable transition for observations of charge exchange recombination radiation from hydrogen-like impurities He^{+}, C^{+5}, O^{+7} have upper principal quantum levels above the n-level at which the partial charge exchange capture cross-sections peak. The partial cross-sections at high n are not well known theoretically and are very sensitive to neutral beam particle energies, E, for $E \lesssim 40$ KeV/amu. Also at JET densities, fields and beam energies, the populations of such high levels are influenced by cascade and by redistributing transitions (especially in ℓ) due to collisions with plasma ions and/or dynamic field effects. Figure 7 shows comparative theoretical cross-sections for $H(1s) + O^{+8} \rightarrow O^{+7}(n) + e$.(Spence and Summers, 1986). If charge exchange recombination from H(1s) is the sole primary populating mechanism, then the column emissivity of a spectrum line excited by charge exchange recombination, I,

may be written as

$$I = q_{eff} \int N(H(1s))N(A^{+z}o)dl$$

where q_{eff} is an effective rate coefficient for the transition averaged over the interaction region and the line integral is the 'charge exchange emission measure'. In principle, a measurement of m spectrum line column emissivities with upper levels lying between n_{min} and n_{max} can yield the emission measure and experimental to theoretical direct charge exchange capture rate coefficient ratios for the m upper levels. This is with the constraint that the sum of experimental and theoretical direct charge exchange capture rate coefficients over the m levels are made equal - a more confident constraint that correctness of individual theoretical partial charge exchange capture coefficients. These results are not immediate since l-level mixing and cascade from higher levels confuses the simple connection. We have established computational methods for transferring the influence of all levels onto the set m using a theoretical model and matrix condensation techniques (Peacock et al. (1986). - to be published). More details of the data on reaction rates, energies etc. used in the theoretical model can be found in Spence and Summers (1986).

Figure 8 shows predicted column emissivities and line shapes for some principal quantum shell transitions of O^{+7} based on an observed column emissivity for the 10-9 transition in JET. Some analysis of He^{+} charge exchange radiation observed on the ASDEX tokamak (for which three unblended lines are measurable) has been carried out. q_{eff} from our model is in reasonable agreement with Fonck et al. (1984). Initial indications are that deduced emission measure is consistent with beam attenuation and plasma impurity distribution expectations. The experimentally inferred direct charge exchange recombination rate coefficient variation with n is slightly shallower than the theoretical UDWA (Ryufuku, 1982) model suggests. The ratio of emission measures for different

elements may reasonably be interpreted as relative concentrations of the elements in the interaction region. Absolute concentrations require a model for the neutral beam attenuation and observation geometry. Figure 9 shows some results in JET. Further details are given in Von Hellerman et al. (1986).

REFERENCES

Behringer, K H (1986) Proc.7th Int.Conf. on Plasma-Surface Interactions in Controlled Fusion Devices, Princeton, USA. (in JET Joint Undertaking report JET - P(86)35).

Behringer, K H (1986) Rev.Sci.Instrum.57, 2000.

Behringer, K H and Summers, H P (1987) - to be published.

Fonck, R et al. (1984) Phys.Rev.29, 3288.

Fritsch, W (1984) Phys.Rev.A30, 3324.

Fritsch, W and Lin, C D (1984) Phys.Rev. A29. 3034.

Janev, R K and Bransden, B H (1982) Int.Nucl.Data.Comm. Report INDC(NDS)-135/GA.

Janev, R K, Bransden, B H and Gallagher, J W (1983) J.Phys. Chem.Ref.Data 12, 829.

Peacock, N J, Summers, H P and Von Hellermann (1987) - to be published.

Ryufuku, H (1982) Japan.Atom.Energy Research Inst. report JAERI-M-82-031.

Salop, A (1979) J.Phys.B.12, 919.

Shipsey, E J, Green, T A and Brown, I C (1983) Phys.Rev.A27, 821.

Spence, J and Summers H P (1986) J.Phys.B19, 3749.

Von Hellerman, M G, Boileau, A, Horton, L D, Summers, H P and Peacock, N J (1986) Proc.Workshop on Basic and Adv.Fusion Plasma Diag.Techniques, Varenna, Italy.

Table 1 Metastable states of Cr^{+1} and spectrum lines suitable for influx analysis.

Ion	Metastable term	Index
Cr^{+1}	$3d^5\ {}^6S$	1
	$3d^5\ {}^4G$	2
	$3d^4({}^5D)4s\ {}^6D$	3
	$3d^4({}^5D)4s\ {}^4D$	4
	$3d^4({}^3H)4s\ {}^4H$	5
	$3d^4({}^3H)4s\ {}^2H$	6

Ion	Multiplet Index	Transition Multiplet	Component	λ(Å)	Branching ratio	Metastable Index	A-value (sec^{-1})
Cr^{+1}	α	$3d^5\ {}^6S-3d^4({}^5D)4p\ {}^6P$	5/2- 7/2	2055.59	0.40	1	1.97[a]
						3	2.93[a]
	β	$3d^5\ {}^4G-3d^4({}^3H)4p\ {}^4G$	11/2-11/2	2133.50	0.46	2	1.94[a]
						5	2.05[a]
	1	$3d^4({}^5D)4s\ {}^6D-3d^4({}^5D)4p\ {}^6F$	9/2-11/2	2835.62	1.0	3	2.76[a]
	7	$3d^4({}^5D)4s\ {}^4D-3d^4({}^5D)4p\ {}^4F$	7/2-9/2	3132.03	0.83	4	1.92[a]
	14	$3d^4({}^3H)4s\ {}^4H-3d^4({}^3H)4p\ {}^4I$	13/2-15/2	2822.37	1.0	5	2.70[a]
	25	$3d^4({}^3H)4s\ {}^2H-3d^4({}^3H)4p\ {}^2I$	11/2-13/2	3050.12	0.78	6	1.8[a]

Table 2 Carbon and oxygen limiter fluxes at 100 eV relative to hydrogen.

Metastable ion	Γ/Γ_H(%)	
O^{+1} $2s^2 2p^3$ ^4S	.74	1.6
$2s^2 2p^3$ ^2D	.60	
$2s^2 2p^3$ ^2P	.25	
O^{+2} $2s^2 2p^2$ ^3P	.84	1.4
$2s^2 2p^2$ ^1D	.37	
$2s^2 2p^2$ ^5S	.23	
C^{+1} $2s^2 2p$ ^2P	7.7	9.1
$2s\ 2p^2$ ^4P	1.4	
C^{+2} $2s^2$ ^1S	2.4	5.9
$2s2p$ ^3P	3.5	

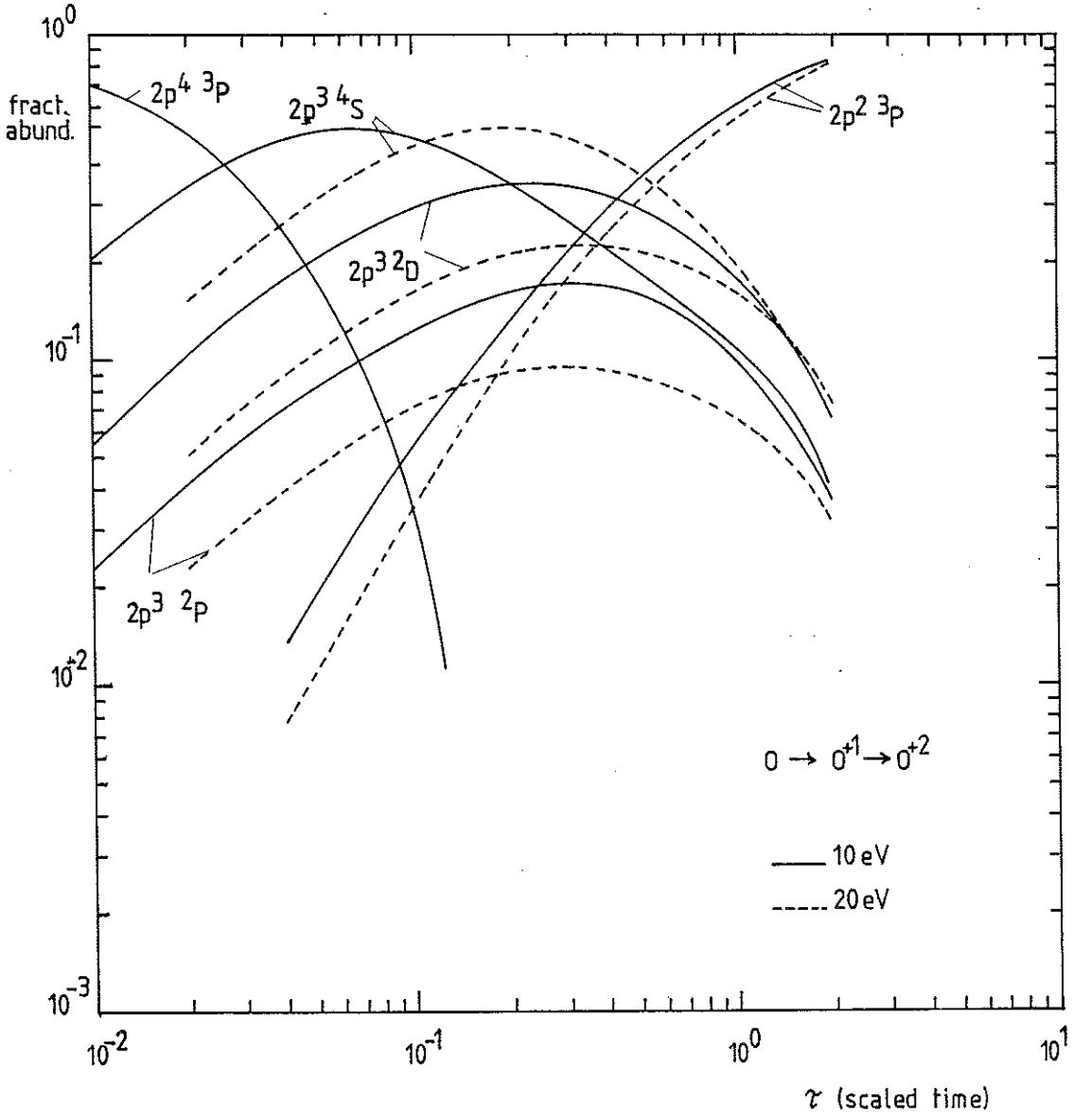

Figure 1 Fractional abundances of metastable states of O^{+1} in time dependent ionisation at fixed electron density and temperature. It is assumed that the ionisation commences with ions in the ground state of O and evolves to the ground state of O^{+2}.

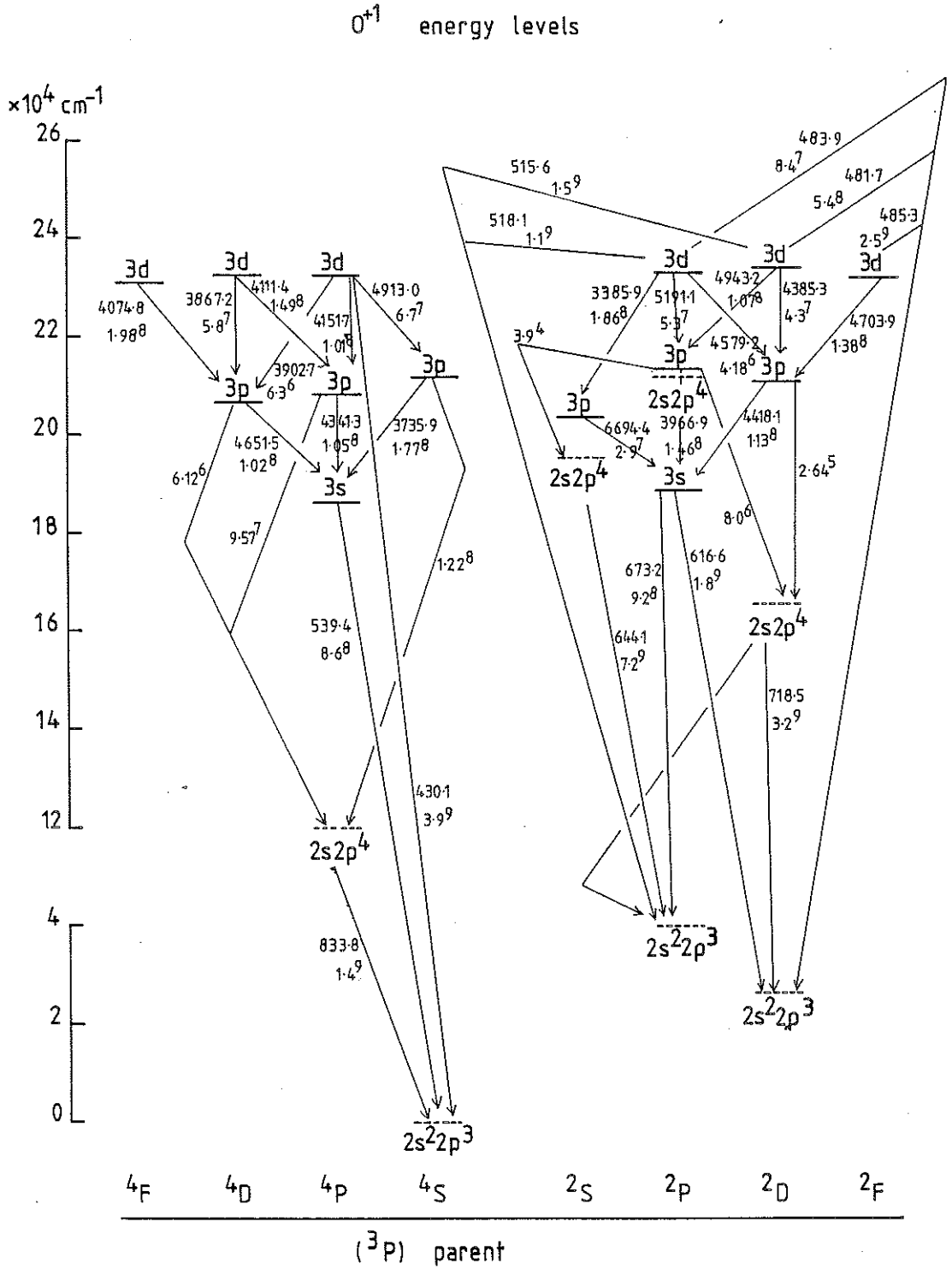

Figure 2 Energy level diagram of excited states of O^{+1} considered in the population calculations for influx determination. Transition multiplet wavelengths (A) and transition probabilities (sec^{-1}) are given. The multiplets used for influx analysis are (1) 3735.9 A, (2) 3966.9 A, (3) 4418.1 A.

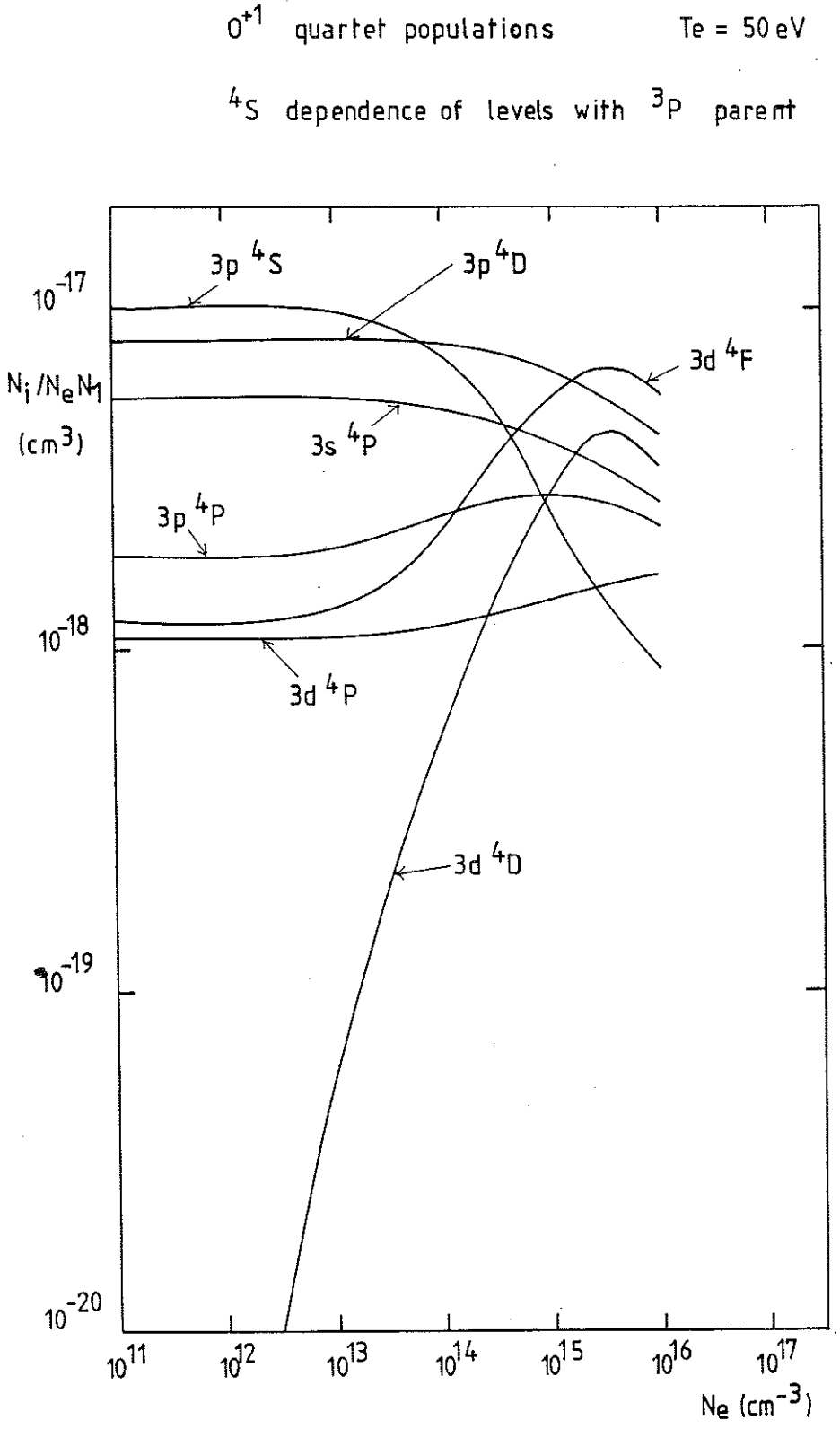

Figure 3 Behaviour of excited quartet populations of O^{+1} with density at fixed temperature. The dependence of the populations of excited levels i on the ground state 1 ($2p^3$ ^4S) only is shown. That is the other metastable states are assumed depopulated.

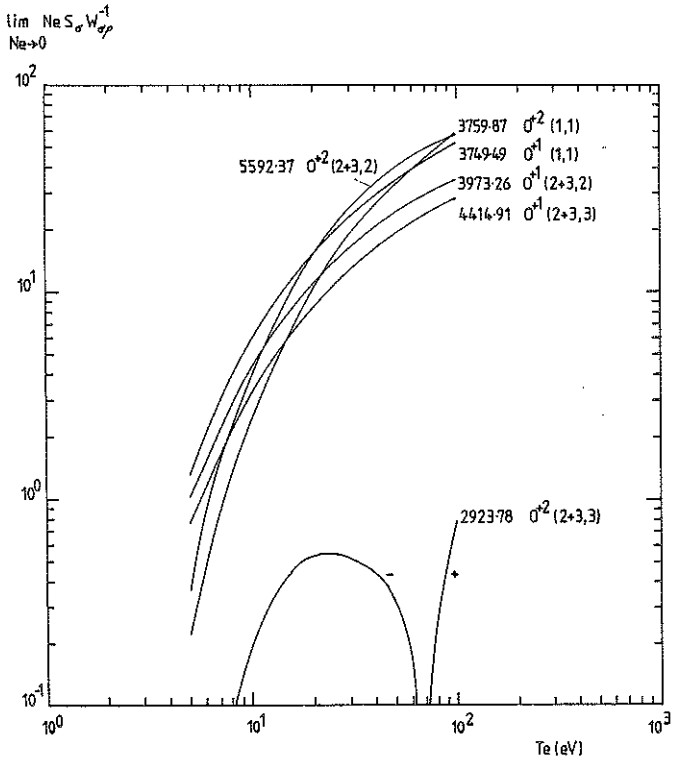

Figure 4 Ionisation/photon curves for O^{+1} and O^{+2} at zero density. The various measurable line of sight emissivities are indicative of the fluxes in particular metastable states as shown. The metastable states of O^{+1} are (1) $2p^3\ ^4S$, (2) $2p^3\ ^2D$, (3) $2p^3\ ^2P$ and of O^{+2} are (1) $2p^2\ ^3P$, (2) $2p^2\ ^1D$, (3) $2p^2\ ^1S$. The O^{+1} lines are components of the multiplets given in figure 2.

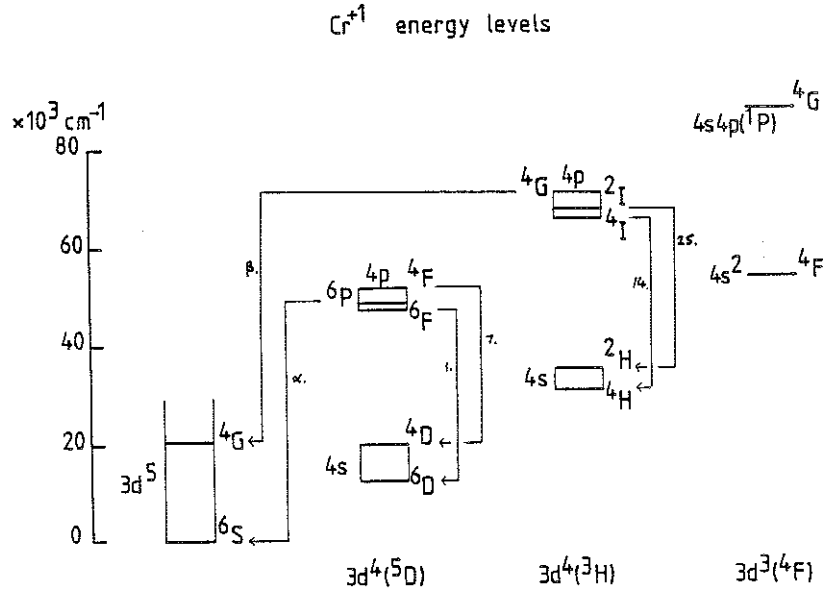

Figure 5 Energy levels and spectrum lines used for analysis of the influx of Cr^{+1} in various metastable states.

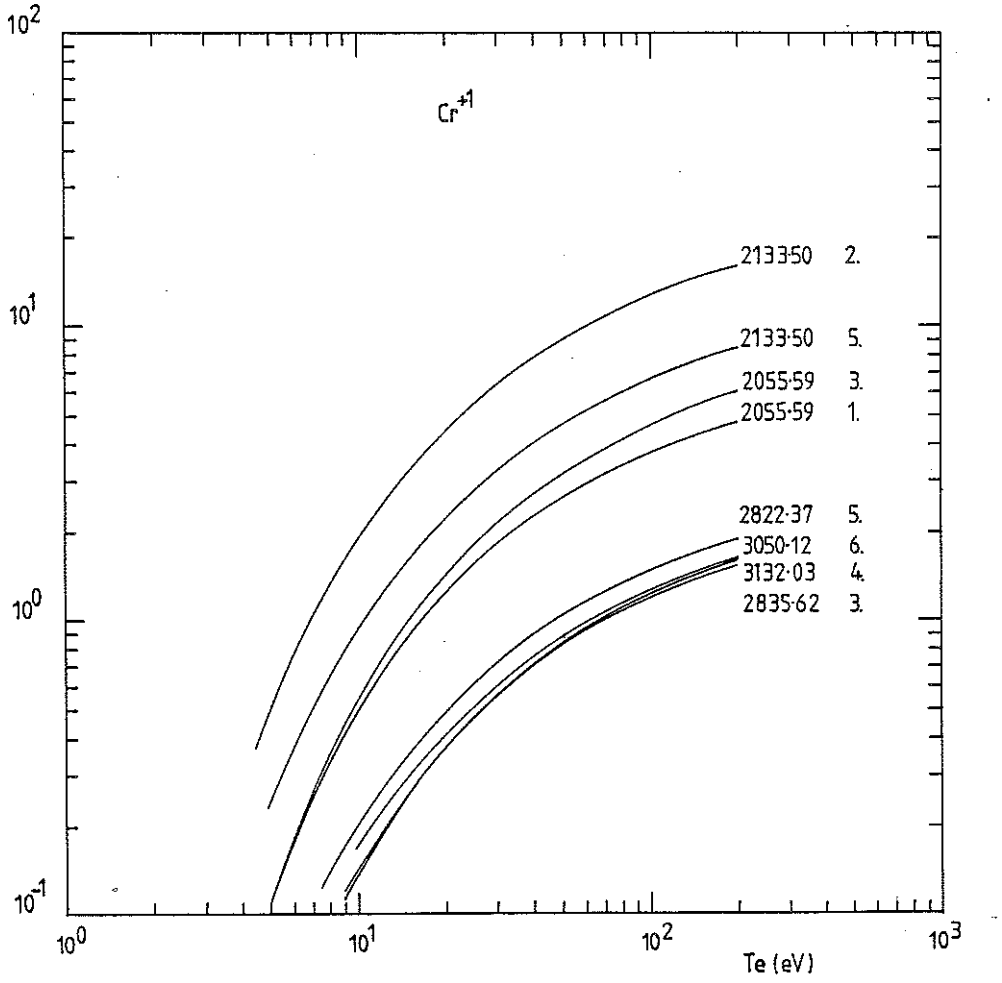

Figure 6 Ionisation/photon curves for Cr^{+1} at zero density. The lines and metastable states are specified in table 1.

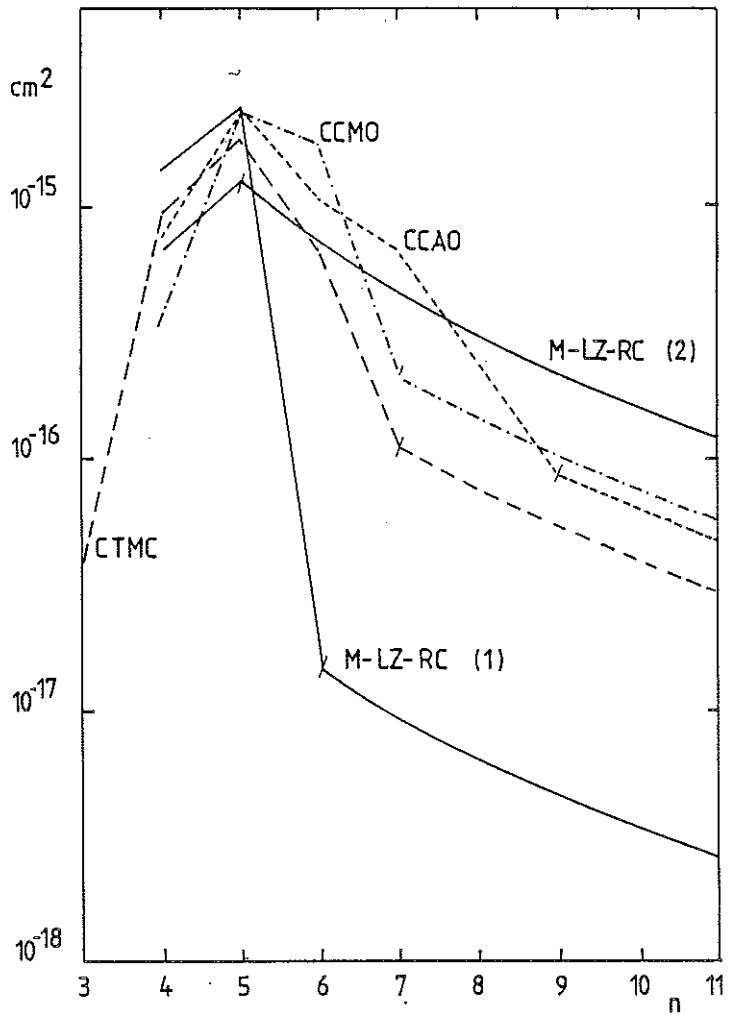

Figure 7 Comparison of partial charge exchange cross-sections σ_n to excited quantum shells n of O^{+7} in the reaction $H(1s) + O^{+8} \rightarrow p + O^{+7}(n)$. The hydrogen atoms form a monoenergetic beam of energy E_H = 25 KeV. Source data is extrapolated beyond its range assuming a $1/n^3$ behaviour

CCAO - (Fritsch, 1984; Fritsch & Lin, 1984)

CCMO - (Shipsey et al, 1983: see also Janev et al, 1983)

CTMC - (Salop, 1979)

M-LZ-RC - (Janev et al, 1982; Janev et al, 1983)

(1) $1/n^3$ form from largest n value

(2) $1/n^3$ form from n_{crit}

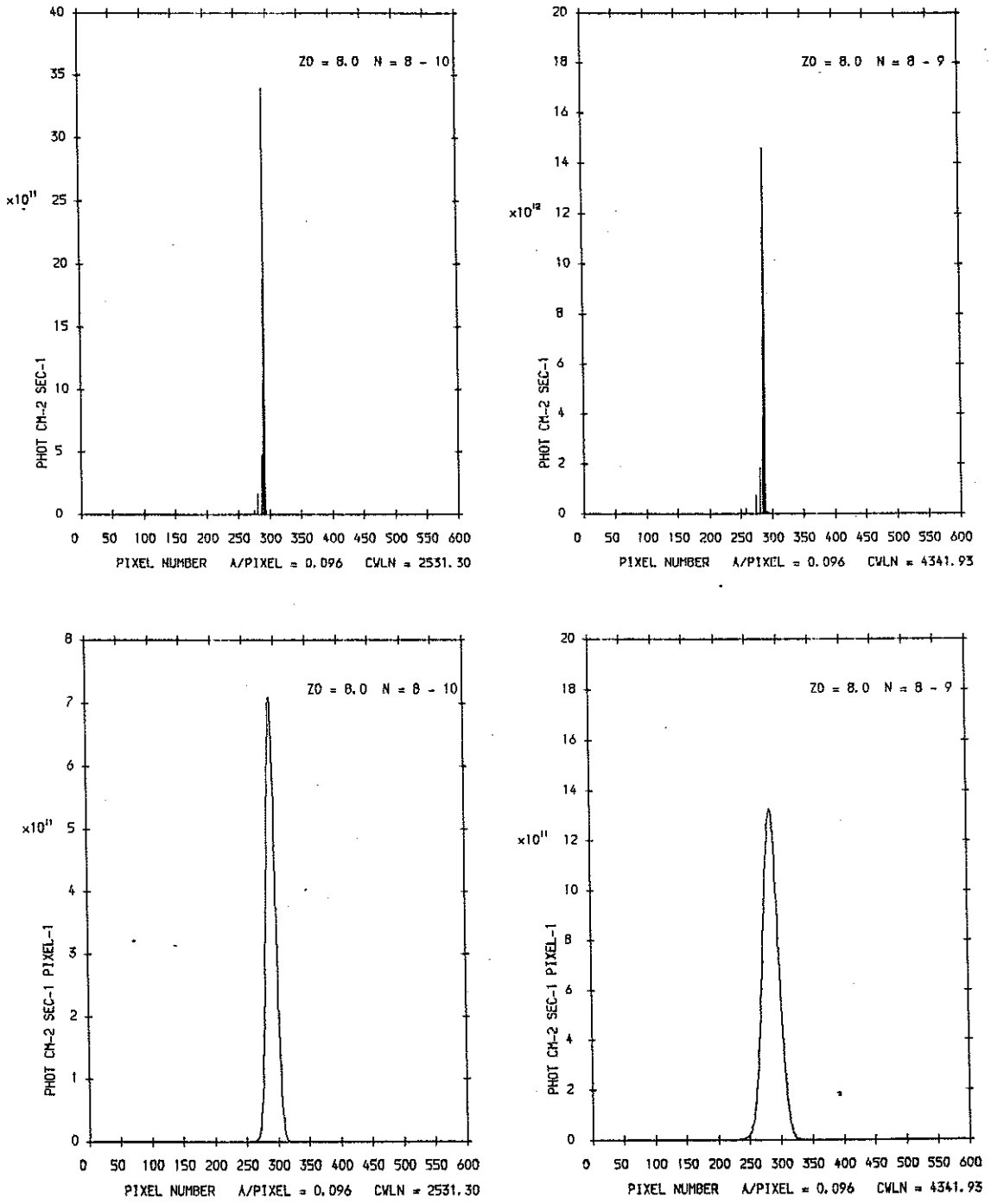

Figure 8 Predicted column emissivities and line profiles for some charge exchange lines of O^{+7}. The n=10-9 line column emissivity is observed in JET. The component emissivities, Doppler broadened line profiles, emissivities for other transitions and the emission measure are deduced.

T_e = 1 keV, T_i = 1 keV, $N_e = 2.0^{13}$ cm^{-3}, $N_i = 7.0^{12}$ cm^{-3}, Z_{eff} = 3, E_H = 50 keV. Column emissivity for n=10-9 = 2.0^{13} $ph.cm^{-2}$ sec^{-1}. Emission measure = 1.8^{21} cm^{-5}.

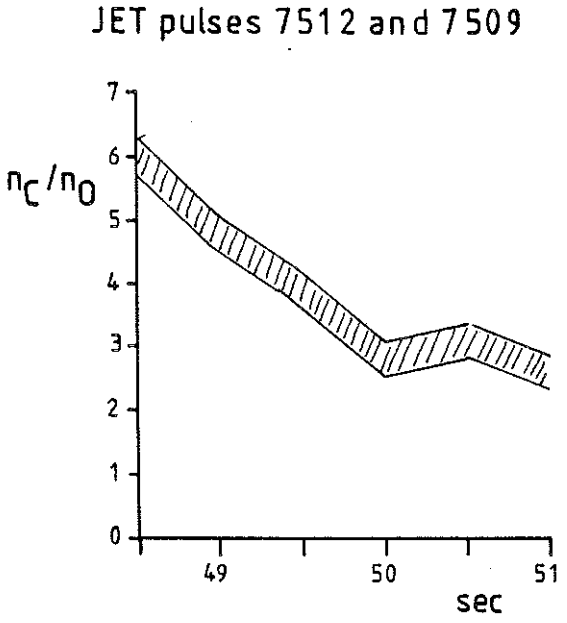

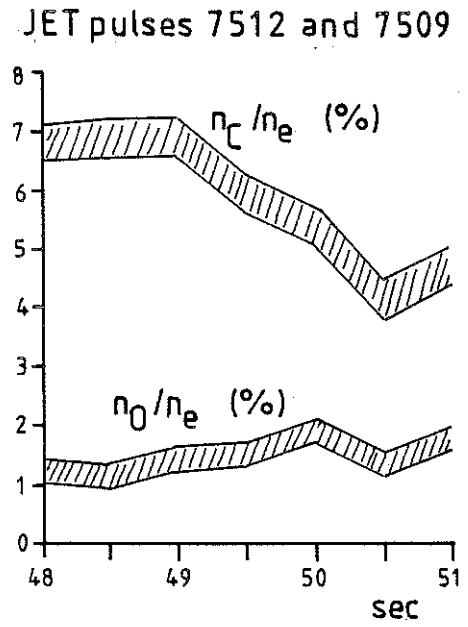

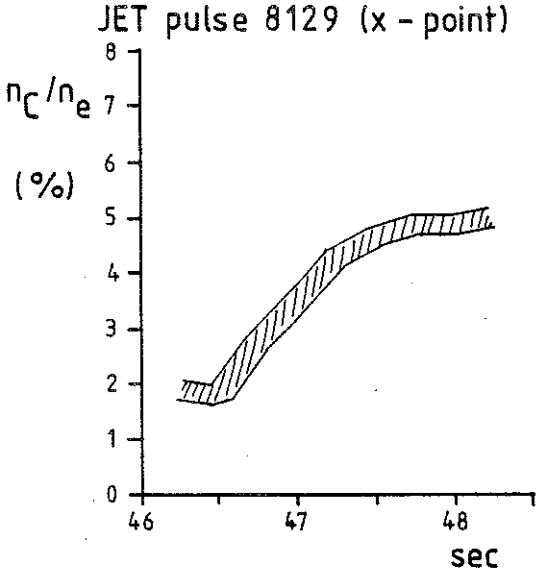

Figure 9 Central densities of carbon and oxygen impurities in three JET discharges deduced using charge exchange recombination spectroscopy.